Geo-Marine Letters (2024) 44:14
https://doi.org/10.1007/s00367-024-00776-3

REVIEW

The concept of wave base: fact and fiction

B. W. Flemming[1]

Received: 29 April 2024 / Accepted: 31 July 2024

Abstract
This study focusses on the processes that control the morphodynamics of the seabed in the shoaling wave domain, widely known as the shoreface. Shoreface morphodynamics is not only controlled by the local wave climate but also by associated wave- and wind-driven currents, the grain-size, and antecedent geomorphology. This paper provides basic information on sedimentological action of monochromatic waves at the seabed in the shoaling zone to the non-specialist without him-/herself having to solve the complex equations before arriving at workable solutions. It is emphasized that the traditional oceanographically defined wave base ($0.5L_0$) is not relevant in a geological/sedimentological context and should be replaced by a grain-size dependent effective wave base (EWB). Furthermore, open ocean swell-dominated shorefaces have to be distinguished from those of marginal seas dominated by local wind-generated waves. For convenience, a collection of tables and diagrams are provided in the electronic supplementary material (ESM) attached to this paper. They highlight the depths of effective wave bases for a range of grain sizes, wave heights and wave periods between 2 and 16 s.

Keywords Shoaling zone · Shoreface · Wave height · Wave period · Oceanographic wave base (OWB) · Effective wave base (EWB) · Fair-weather wave base (FWWB) · Storm wave base (SWB)

Introduction

An enigmatic parameter frequently encountered in the marine geoscience literature is the so-called *wave base*. This parameter, however, is highly ambiguous because it has a different meaning to different people. Thus, in physical oceanography the wave base is defined as the water depth that corresponds to one-half of the deep-water wavelength ($d_{wb} = 0.5L_0$, where $L_0 = 1.56T^2$) (e.g. Komar 1998; Masselink et al. 2011). At this depth a wave is said to 'feel' the bottom and hence begins to lose energy by friction along the seabed. The oceanographic wave base is thus simply a function of the wave period and the associated deep-water wavelength, and is hence independent of the physical nature of the seabed. In older marine geoscience literature (e.g. Shepard 1963) the oceanographic wave base (OWB) has generally been interpreted as representing the water depth marking the onset of offshore sediment disturbance. As a reminder, the orbital velocity of waves decreases exponentially with water depth and approaches zero at the depth corresponding to the deep-water wavelength (L_0). At the depth of the OWB ($0.5L_0$) the orbital velocity is approximately 4% of that at the sea surface (e.g. Shepard 1963) and is the depth at which wave energy at the seabed begins to measurably decrease due to friction (Fig. 1). The OWB of course changes in response to changes in the seasonal wave climate, e.g. fair-weather vs. storm season, whereby the depth varies more strongly in the latter season because of a more variable wave spectrum.

The wave base concept is generally applied to the shoaling wave domain where waves dissipate their energy by friction along the seabed. It is widely known as the shoreface, which occupies the space between the surf zone and the depth of the OWB. Wave energy dissipation increases as water depth decreases and waves can hence move progressively coarser-grained sediment the shallower the water becomes. In nature the processes affecting the seabed are controlled by the local wave climate, wave and wind-driven currents, the antecedent geomorphology, the seabed slope, and the grain-size of the sediment. The interactions between these factors are complex and vary strongly from place to place.

✉ B. W. Flemming
bflemming@senckenberg.de

[1] Senckenberg am Meer, Marine Research Department, Südstrand 40, 26382 Wilhelmshaven, Germany

Published online: 27 August 2024

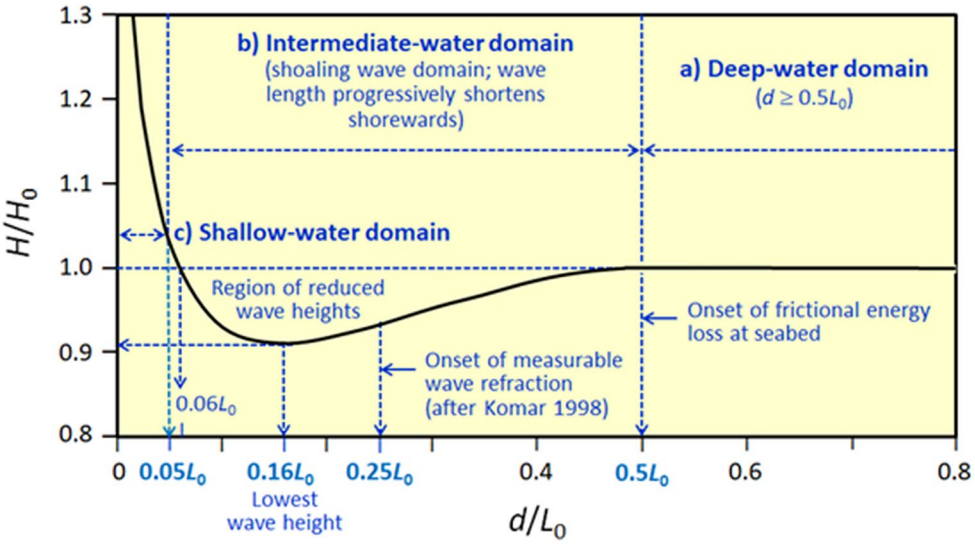

Fig. 1 Evolution of dimensionless wave height (H/H_0) in the course of wave shoaling (d/L_0)

Ocean waves are rarely monochromatic but mostly consist of numerous superimposed wave trains of different period, height and direction (cf. Collins 1976). For these reasons, generalized predictions of seabed responses cannot be made, except perhaps in simple, straightforward cases. To this day, this complexity is mirrored in a constant flow of papers, special issues and textbooks dealing with shoreface processes in a broader sense, e.g. Bascom (1964), McCave (1971), Komar and Miller (1973), Clifton (1976), CERC (1984), Clifton and Dingler (1984), Allen 1985, 1994), Horikawa (1988); Hardisty (1994), Wright (1995), Soulsby (1997), Komar (1998), Short (1999), Dean and Dalrymple (2004), Le Roux (2008), Immenhauser (2009), Davidson-Arnott (2010), Masselink et al. (2011), Valiente et al. (2019); Anthony and Aagaard (2020), Hamon-Kerivel et al. (2020) and, most recently, Jackson and Short (2020) and Bosboom and Stive (2023).

Modern reviews of essential wave parameters can, for example, be found in Collins (1976) and Bryan and Power (2020). Tables of maximum horizontal, wave-generated velocities at the seabed (U_{max}) can be found in CERC (1984), although unfortunately in non-metric Imperial units, which then require conversion from the FPS (foot/pound/second) system to the metric MKS (metre/kilogram/second) or SI system. Computer-generated metric options are provided by Wiberg and Sherwood (2008) and Le Roux et al. (2010). A popular handbook providing quantitative approaches to the study of marine sand dynamics, including worked-out solutions, is that of Soulsby (1997).

This paper has two major objectives: (a) to provide some basic information on wave transformation and its sedimentological action at the seabed in the shoaling zone to the non-specialist working in this domain (e.g. biologists, geographers, geologists) without him-/herself having to solve all the complex equations before arriving at workable solutions; (b) to highlight the need for a stricter and geologically meaningful definition of the wave base concept. It is emphasized that the solutions presented in this paper strictly apply to siliciclastic sediments of density $\delta = 2.65$ g cm^{-3}. Bioclastic sediments, which are characterized by multiple grain shapes, are explicitly excluded.

Methods

Essential parameters, dimensions and functions

L_0 is the deep-water wavelength ($gT^2/2\pi$ or $1.561T^2$) in metres (m), L the shoaling wavelength (m), T the wave period (s), H the wave height (m), d the water depth (m), D the grain size (mm), g the gravitational acceleration (9.81 m/s^2); $\pi = 3.1416$, sinh the hyperbolic sine, tanh the hyperbolic tangent, U_{max} the maximum horizontal velocity (m/s) close to the seabed, and U_{crit} the threshold velocity for the initiation of sediment movement at the seabed involving siliciclastic sediment composed of variable mean grain sizes. It should be noted that, for simplicity, the wave data discussed in this paper strictly relate to monochromatic waves of the sinusoidal type (linear Airy wave theory). As waves in nature are random and irregular, T and H are understood to represent the peak spectral wave period (T_p) and the significant wave height (H_s), respectively.

Shoaling wave parameters

As deep-water waves propagate shoreward, they eventually reach a water depth where they 'feel' the bottom, the ensuing friction resulting in increasing energy loss with decreasing water depth. In this scenario one distinguishes between three domains:

a) A deep-water domain where $d \geq 0.5L_0$;
b) An intermediate-water domain occupying the zone between $d \leq 0.5L_0 \geq 0.05L_0$; and.
c) A shallow-water domain beginning at the depth corresponding to $d \leq 0.05L_0$.

The above relationships are illustrated in Fig. 1 in which the dimensionless wave height (H/H_0) is plotted against the dimensionless water depth (d/L_0). Note that, due to friction along the seabed, the wave height progressively decreases from a depth of ~$0.5L_0$ up to a water depth corresponding to d=~$0.16L_0$, where the waves reach their smallest height (H/H_0=~0.91). Thereafter their height increases sharply due to rapid steepening caused by the rapid decrease in wave celerity in shallow water (shoaling effect).

Additional functional wave parameters

In deep water, the maximum wave height is limited to 1/7 of the deep-water wavelength (L_0):

$$H_{\max} =\sim 0.1429L_0 \tag{1}$$

For any wave period the maximum wave height in deep water also defines the maximum wave height that may occur at the onset of frictional energy loss at the seabed (i.e. at d=$0.5L_0$; cf. Figure 1).

In very shallow water, defined as ≤$0.05L_0$, $U_{\max}$ for any wave height and water depth is no longer governed by the wavelength and wave period, but only by the gravitational acceleration:

$$U_{\max} = .5H \times (g/d)^{0.5} \tag{2}$$

Furthermore, waves eventually break when the orbital velocity becomes larger than the wave celerity in the course of shoaling (e.g. Bosboom and Stive 2023). The critical depth in relation to the wave height (and vice versa) is calculated by:

$$d = 1.282H \tag{3a}$$

or

$$H = 0.78d \tag{3b}$$

Calculation of U_{crit} under waves

The calculation of the critical threshold velocity, i.e. the velocity required for the initiation of sediment movement for a given grain size as a function of a given wave period, and the maximum horizontal velocity at the seabed for a given wave height and water depth as a function of the wavelength at that depth, is achieved in three steps:

Step 1: The critical wave-generated threshold velocity (U_{crit}) for any grain size (D) expressed in mm as a function of a given wave period (T) (cf. Komar and Miller 1973) can be determined by consulting Soulsby (1997), or by applying the empirical trend-surface equation of Flemming (2005; based on the digitization of the corresponding figure in Clifton 1976; his Fig. 4).

$$U_{crit} = \left(5.1325 + 27.4576D + 0.2849D^2 + 0.0909T\right) / \left(1 + 0.344D + 0.004D^2 - 0.0638T + 0.002T^2\right) \tag{4}$$

where U_{crit} is the critical threshold velocity in cm/s, D is the grain size in mm, and T is the wave period in seconds. Close approximations of U_{crit} values in m/s for selected grain sizes and wave periods are listed in the Electronic Supplementary Material (ESM) attached to this paper (ESM Table 1), together with the source diagram of Clifton (1976) (ESM Fig. 1a), the trend surface diagram of Flemming (2005) (ESM Fig. 1b) and a statistical comparison between the two (ESM Fig. 1c).

Step 2: Once the critical threshold velocity for any specified grain size and wave period is known, it is necessary to determine the maximum orbital velocity ($U_{\max}$) for the specified water depth and the wavelength (L) at that water depth. In this way it can be determined at what water depth U_{crit} is reached for a specific grain size along a wave orthogonal. $U_{\max}$ can be determined by means of the following equation.

$$U_{\max} = (\pi H/T) \times 1/\sinh(2\pi d/L) \tag{5}$$

where $U_{\max}$ is the maximum horizontal velocity at the seabed (m/s), H is the wave height (m), sinh is the hyperbolic sine, d is the specified water depth (m), π=3.1416, and L the wavelength (m) for period T (s) at that water depth. However, to solve Eq. 5, the wavelength L at the specified water depth must first be determined.

Step 3: In the shoaling zone the wavelength L decreases with decreasing water depth while the wave period remains unchanged. At the specified water depth (in Eq. 5) L can be determined by a number of different approaches, e.g. by solving the following equation.

$$L = 1.561T^2 \times \tanh(2\pi d/L) \tag{6}$$

where $1.561T^2$ represents the deep-water wavelength (L_0) derived from $L_0 = gT^2/2\pi$ with g as the gravitational acceleration (9.81 m/s^2), tanh as the hyperbolic tangent, and the remaining parameters as defined before. As L is contained

on both sides of the equation, its value has to be determined by iterative (trial and error) approximation.

Alternatively, L can be derived from the Excel-VBA spreadsheet WAVECALC of Le Roux et al. (2010), or from mathematically simplified forms of Eq. 6 provided by Soulsby (1997):

$$L = T(gd)^{0.5}/\{1 + (4\pi^2 d)/(5T^2 g)\} \quad \text{valid for } \pi^2 d/T^2 g \leq 0.25 \tag{7a}$$

and

$$L = T\left(gT^2\right)/2\pi[1 + 0.2^{\{2-(8\pi 2d)/(T2g)\}}] \quad \text{valid for } \pi^2 d/T^2 g \geq 0.25 \tag{7b}$$

To decide which of the two options applies, the limiting criterion $(\pi^2 d)/(T^2 g)$ ≤0.25 or ≥0.25 has to be checked in each case. When correctly applied, the deviations amount to < 1% of the values obtained by the iteration procedure (cf. ESM Table 2).

In this context it should be pointed out that Immenhauser (2009) attempted to solve Eq. 6 for the water depth (d) with the aim of simplifying palaeo-environmental interpretations. This attempt, however, failed for two reasons: (a) the rearranged equation (his Eq. 10) is mathematically incorrect, and (b) even in its correct form it would be nonsensical because in order to determine d the a priori knowledge of L (and vice versa) is required because the two parameters are intimately linked.

The relationship between water depth and the length of shoaling waves for a variety of wave periods is illustrated in Fig. 2a and b. The curves for all wave periods show that frictional energy loss is minimal up to a water depth corresponding to ~$0.5L_0$ (viewed from right to left). From the water depth of $0.5L_0$ (OWB) onward the curves begin to become progressively steeper, i.e. the wavelength rapidly becomes shorter as water depth decreases further.

Transition to upper plane bed conditions

The transition from lower to upper regime bedload transport under waves, i.e. from hummocky/swaley cross-bedding to upper plane bed transport (sheet flow), is only dependent on the particle diameter and independent of the wave period (cf. ESM Fig. 1d; based on Clifton 1976). It can be approximated by the relation:

$$U_{\text{upb}} \approx 1.97(D_{\text{mm}})^{0.5} \tag{8}$$

where U_{upb} is the critical upper plane bed velocity (m/s) and D_{mm} is the grain diameter in mm. Selected upper plane bed velocities for a variety of grain sizes are listed in ESM Table 3.

Depth of closure

The depth of closure is the seaward depth limit of measurable offshore/onshore sediment transport, which corresponds to the foot of the so-called upper shoreface sand prism (e.g. Wright et al. 1991). A thorough discussion of the depth of closure concept has recently been presented by Valiente et al. (2019). Besides the depth of closure (DoC), they have also identified a maximum water depth of sediment movement (DoT), which can probably be equated with the EWB of the present paper. Sediment moved across the DoC is not commonly returned to the shore by wave action alone and is hence frequently lost from the upper shoreface sediment compartment. A widely applied equation for the closure depth is that of Hallermeier (1978, 1981; cf. also Valiente et al. (2019) and Hamon-Kerivel et al. 2020):

$$d_{\text{cl}} = 2.28H_{\text{s}} - 68.5(H_s^2/\text{g}T_s^2) \tag{9}$$

where d_{cl} is the closure depth (m), H_{s} is the significant wave height (m), T_{s} the significant wave period (s) and g the

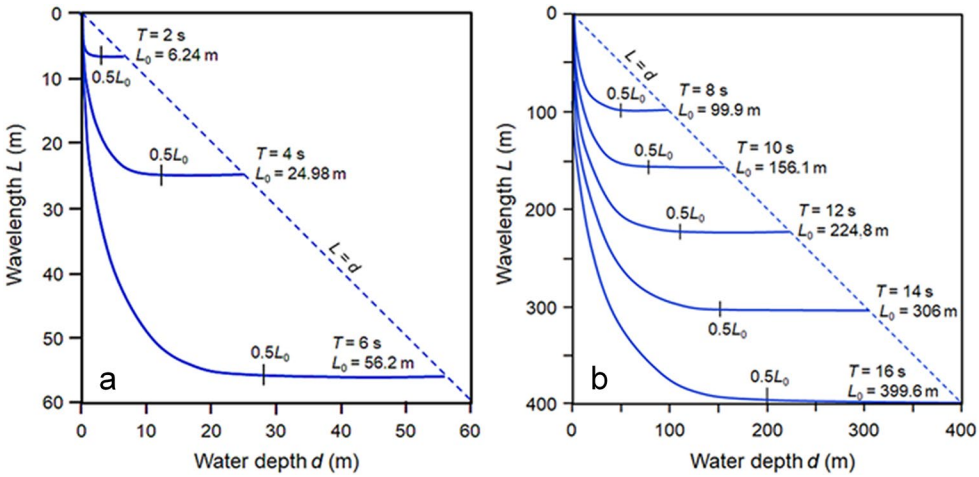

Fig. 2 Wavelengths of shoaling waves as a function of water depth and wave period: (**a**) Wave periods of 2, 4 and 6 s. (**b**) Wave periods of 8, 10, 12, 14 and 16 s

acceleration due to gravity (9.81 m/s). Solutions for selected wave periods and wave heights are listed in ESM Table 4.

Results and discussion

Practical applications

From a modern marine geological/sedimentological perspective the depth at which siliciclastic sediments of particular mean grain sizes begin to be stirred by gravity waves is a function of the regional wave climate, i.e. of the peak wave period and significant wave height that characterize a particular geographic location (e.g. McCave 1971). It stands to reason that different mean grain sizes will begin to move at different water depths, quite independently of the depth of the OWB. This is illustrated in Fig. 3 for 8 s waves (vertical blue lines). To distinguish these depths from the oceanographic wave base, one should preferentially speak of a grain-size dependent *effective wave base* (EWB) (Flemming 2005). As already pointed out by Dietz (1963) and most recently by Rankey and Appendini (2022), the OWB concept is, in this context, basically meaningless, its distinction from an EWB being widely ignored in the marine geosciences.

In this connection it has become popular to distinguish between a so-called 'fair-weather wave base' (FWWB) and a 'storm wave base' (SWB), the two being generally associated with specific sedimentary facies changes on ancient and modern shorefaces (e.g. Hobday and Reading 1972; Burchette and Wright 1992). Whether the distinction between fair-weather and storm wave bases is stratigraphically at all relevant has in more recent years been called into question (Peters and Loss 2012). Nevertheless, up to the present day the majority of marine geoscientists neither identify which type of wave base (EWB or OWB) they are referring to, nor do they cite the source of their terminological choice, rare exceptions being Walker and Plint (1992) and, more recently, also Pellegrini et al. (2023), both having identified the OWB ($0.5L_0$) as their reference depth. These authors (and many others) appear to be oblivious of the conceptual error they introduce into the interpretation of their observations and the process-response models developed on that basis.

As shown in Fig. 3, the effective wave base for particles of varying grain size (here for 8 s waves) varies as a function of wave height. In effect, finer-grained particles begin to move at greater water depths than coarser-grained ones, the effective depth increasing with increasing wave height (vertical blue lines in Fig. 3), and also with increasing wave period (cf. ESM Tables 5–12 and ESM Figs. 2–9). The same applies to the transition from lower to upper regime conditions (upper plane bed; vertical red lines in Fig. 3 and ESM Figs. 2–9). The diagrams clearly demonstrate that, for a given grain size, the EWB varies greatly as a function of wave height and is basically independent of the OWB.

Diagrams such as Fig. 3 can be used to extract information characterizing the dynamic conditions on a shoreface. This information can then be presented in particular forms that can serve to explain the local sedimentary and

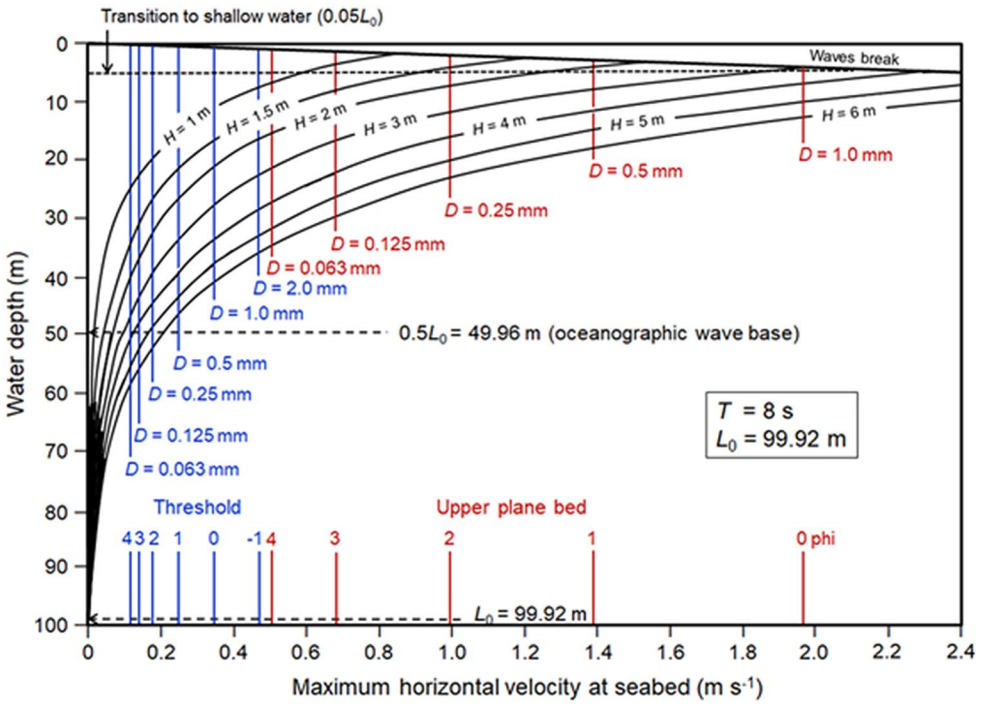

Fig. 3 Maximum horizontal velocities at the seabed (U_{max}) for waves of $T = 8$ s as a function of water depth (d), together with threshold velocities for selected grain sizes (blue) and corresponding values for the transition to upper plane bed conditions (red). Grain sizes in phi according to Wentworth (1922)

morphodynamic situations and has successfully been applied by, for example, Son et al. (2012a, b) to interpret the dynamics controlling the shoreface of the East Frisian barrier-island system located in the southern North Sea. It served a rational interpretation of the primary sedimentary structures in relation to the grain sizes characterizing the shoreface-connected ridge system of that marginal sea region.

It can furthermore be shown that embayed or marginal sea coasts dominated by local wind-generated waves must, in this context, be distinguished from swell-dominated open-ocean coasts. The differences between the two settings are illustrated in Fig. 4 (for marginal sea coasts) and 5 (for open ocean swell-dominated coasts). The diagrams clearly demonstrate that a distinction between effective fair-weather and storm wave bases by means of particular sedimentary structures is not as straightforward as the literature would make us believe (e.g. Flemming 2005; Rankey and Appendini 2022). Indeed, in the case of open-ocean coasts, swell-generated bedforms (and hence associated sedimentary structures) produced during fair-weather occur up to substantially greater water depths than those generated by shorter-period storm waves in the same region. As a consequence, the sedimentary structures produced during fair-weather may obliterate those generated by a prior storm event. Contrary to modern environments this would be difficult to recognize in the rock record, and which can therefore result in serious misinterpretations. In the case of marginal seas, on the other hand, the effect reverses, and it is rather doubtful whether sedimentary structures generated during fair-weather will survive the next storm, i.e. with few exceptions their preservation potential is practically zero.

It is commonly observed that shorefaces are characterized by grain-size gradients from coarser- to finer-grained sediments with increasing water depth. Singular diagrams such as those of Figs. 4 and 5, which are valid for a particular mean grain-size only, are therefore insufficient to represent the conditions on such shorefaces. Multiple corresponding diagrams would have to be constructed to represent the different mean grain sizes at different water depths. This can be achieved by employing the U_{crit} data listed in ESM Table 1 in combination with the tabulated U_{max} data for different water depths associated with the particular wave period appropriate to the study area (ESM Tables 2–12). With reference to Figs. 4 and 5, the horizontal lines separating upper regime from lower regime bed conditions and lower regime conditions from no sediment movement will shift upward for coarser mean grain sizes and downward for finer mean grain sizes.

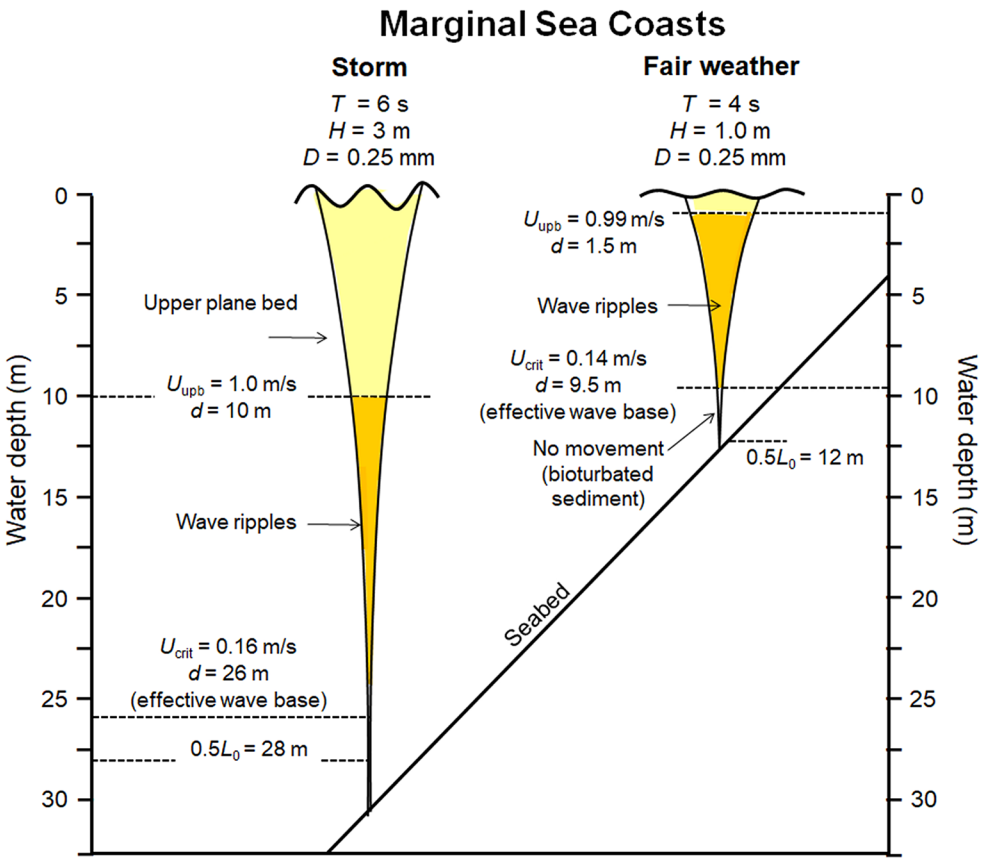

Fig. 4 Comparison of critical velocities (threshold and upper plane bed) for a grain size of 0.25 mm (2.0 phi) under 6 s storm-generated waves and 4 s fair-weather wave conditions along marginal sea coasts for wave heights of respectively 3.0 m and 1.0 m

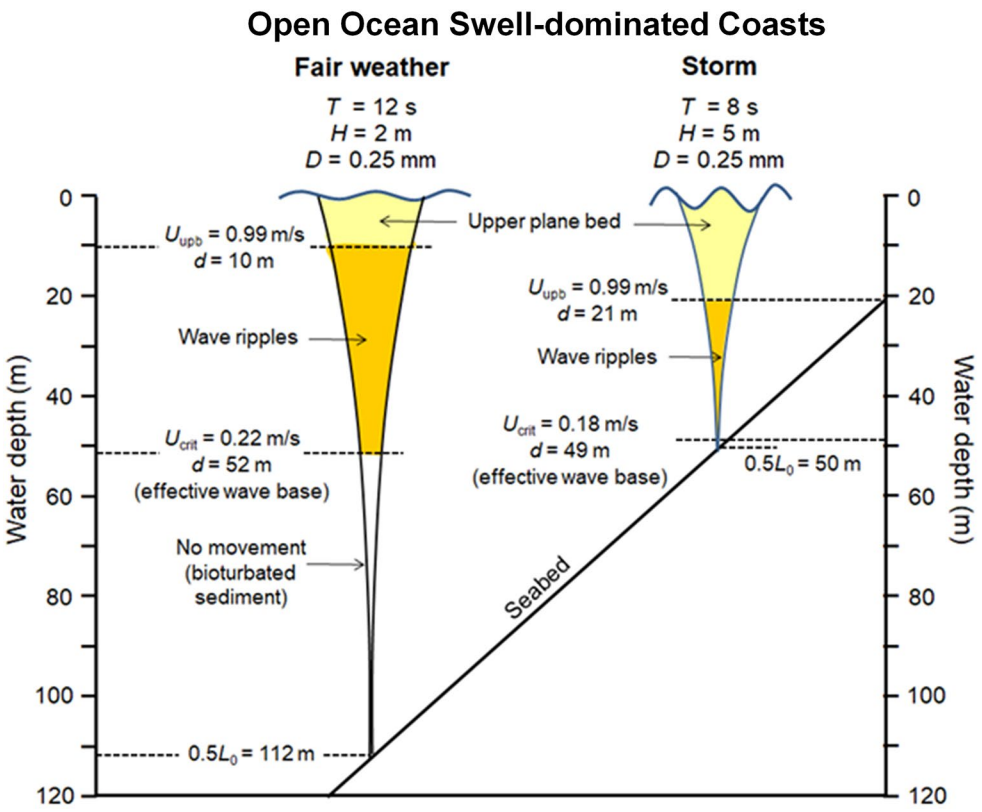

Fig. 5 Schematic comparison of critical wave parameters (threshold and upper plane bed) for a grain size of 0.25 mm (2.0 phi) under 12 s 'fair-weather' swell conditions and 8 s storm-generated waves along open ocean coasts for wave heights of respectively 2.0 m and 5.0 m

Marginal sea coasts

The storm vs. fair-weather condition along marginal sea coasts is illustrated in Fig. 4, which reflects typical storm and fair-weather wave conditions in the southern North Sea (e.g. Son et al. 2012a, b). In marginal seas, storm-generated wave periods and wave heights are always larger than their fair-weather counterparts. In the example illustrated in Fig. 4 the water depths at which U_{crit} for 0.25 mm sands occurs and the depths of the corresponding transitions from lower (wave ripples) to upper regime bedforms (plane bed conditions) are shown. Notable is that during storms the depth of the transition to upper plane bed conditions (14 m) lies below the effective wave base during fair-weather conditions (9.5 m). In effect this means that any sedimentary structures produced by wave-generated ripples during fair-weather conditions will be completely reworked during storms, their preservation potential being practically zero. However, exceptions to this rule can be conceived.

Although sedimentary structures generated during fair-weather will in all likelihood be destroyed by the next storm, there are environmental settings where this may not be the case, Such settings include deltaic environments, where sediment deposition is often decoupled from local storm influences. Thus, high river discharge resulting from heavy rainfall in a distal catchment would supply large amounts of sediment to the coast where, coincidentally, fair-weather conditions happen to prevail, leading to substantial delta-front accretion. In the course, sedimentary structures produced during the prior period of fair-weather conditions can become covered by a variably thick sediment overburden that preserves the underlying fair-weather products. If subsequent storms are unable to completely rework the overlying sediment, any fair-weather sedimentary structures that survive subsequent storm reworking obviously have a fair preservation potential.

Open-ocean swell-dominated coasts

The wave climates of mid- to high-latitudes, especially along the eastern open-ocean margins (west coasts of continents), are generally addressed as high-energy coasts due to the year-round pounding by long-period ocean swells ($T > 8$ s) of variable heights generated by distant high-latitude storms (e.g. Davies 1972). Even during the fair-weather summer seasons these coasts are dominated by such swells (typically 2–3 m high). During the winter season these swell environments are overprinted by shorter-period, locally generated storm waves ($T \leq 8$ s) in the course of passing anticyclonic (northern Hemisphere) or cyclonic (southern Hemisphere) low-pressure cells.

Different seasonal wave climates are at the root of the geological concept that wave-generated sedimentary structures observed at particular water depths will differ between

seasons because of the different wave bases associated with the seasonally different wave climates (Clifton 1976). As a consequence, such sedimentary structures are considered to be diagnostic of either fair-weather or storm conditions preserved in the rock record (e.g. Hobday and Reading 1972; Clifton and Dingler 1984). It is in this context that the generalization of the critical comment about the relevance of the fair-weather vs. storm concept by Peters and Loss (2012) was inappropriate because their wave data was exclusively derived from the east coast of the USA, i.e. from a western ocean margin where the seasonal wave climates are evidently not as different as those observed along eastern open-ocean margins.

Typical seasonal wave climates as, for example, observed along the west coast of South Africa (Woodborne and Flemming 2021) are examined in greater detail in Fig. 5. The diagram schematically highlights the conditions at the seabed for 12 s, 2 m high 'fair-weather' swells (summer season) as opposed to those of 8 s, 5 m high storm waves (winter season). In each case the water depths of the transitions from no sediment movement to lower regime bedforms (ripples), and lower regime bedforms to upper regime bedforms (upper plane bed), together with the critical orbital velocities (U_{crit}) for 0.25 mm sands, are shown. Also indicated are the OWBs for each case, i.e. 112 m for 12 s waves and 50 m for 8 s waves. In the case of the 12 s fair-weather waves the EWB (52 m) for 0.25 mm sand occurs at a greater water depth than that of the storm wave base (49 m). This means that bedforms and associated sedimentary structures produced by the storm waves will in all likelihood be obliterated or be physically reworked by the action of subsequent fair-weather swells.

Conclusions

It has been shown that the oceanographically defined wave base (OWB) has no geological meaning and, as a consequence, should be replaced by an effective wave base (EWB), the depth of which varies as a function of the grain size, the wave period and the wave height. The EWB is probably identical to what Valiente et al. (2019) call the DoT, i.e. "the depth of sediment motion, initiation of vortex ripples and initiation of post-vortex ripples under extreme conditions". In the present paper procedures are proposed of how to determine the EWB for mean grain sizes in the range from − 1.0 phi (2 mm) to 4.0 phi (0.063 mm) as a function of peak wave period and significant wave height together with the associated water depth which can be used to realistically interpret sedimentary environments and facies in both modern shoreface environments and the rock record. In nature, U_{crit}-values for various grain-sizes may differ due to superimposed tidal or wind-driven currents. As the resultant velocity vectors will depend on the strength, direction and angle relative to the direction of the wave orthogonals, corresponding corrections to the positions of the threshold and upper plane bed lines representing various grain sizes (vertical blue and red lines in the d vs. U_{crit} diagrams) would have to be implemented.

Supplementary Information The online version contains supplementary material available at https://doi.org/10.1007/s00367-024-00776-3.

Acknowledgements The author wishes to thank the Senckenberg Natural History Society (Frankfurt) for kindly providing work space and laboratory facilities at their Marine Research Station (Senckenberg am Meer) in Wilhelmshaven, Germany. Eugene Rankey and a second anonymous reviewer are thanked for their critical but constructive comments which served to improve the quality of the paper.

Author contributions BWF is the only author and has generated all the presented data by himself.

Funding Being essentially a theoretical study, the work did not require any outside funding.

Data availability All Data and data -generation procedures are provided within the manuscript or supplementary information files. For convenience, a complete set of tables of maximum horizontal velocities at the seabed together with the associated wavelengths for selected wave periods, wave heights, water depths and selected grain sizes with corresponding graphic displays (analogous to that in Fig. 3) for wave periods from 2–16 s have been added in the Electronic Supplementary Material attached to this paper (ESM Tables 1–12 and ESM Figs 1–8).

Declarations

Competing interests The author declares that there are no competing interests with third parties.

References

Allen JRL (1985) To and fro. In: Allen JRL (ed) Physical sedimentology. George Allen & Unwin, London, pp 243–267

Allen JRL (1994) Fundamental properties of fluids and their relation to sediment transport processes. In: Pye K (ed) Sediment Transport and depositional processes. Blackwell Science, Oxford, pp 25–60

Anthony EJ, Aagaard T (2020) The lower shoreface: Morphodynamics and sediment connectivity with the upper shoreface and beach. Earth Sci Rev 210:103334. https://doi.org/10.1016/J.earscirev.2020.103334

Bascom W (1964) Waves and beaches – the dynamics of the ocean surface. Anchor Books, Doubleday & Co., New York

Bosboom J, Stive MJF (2023) Coastal Dynamics. LibreTexts, Delft University of Technology, Delft

Bryan KR, Power HE (2020) Wave behaviour outside the surf zone. In: Jackson DWT, Short AD (eds) Sandy Beach Morphodynamics. Elsevier, Amsterdam, pp 61–86

Burchette TP, Wright VP (1992) Carbonate ramp depositional systems. Sediment Geol 79:3–57

CERC (1984) Shore Protection Manual. US Army Corps of Engineers. Coastal Engineering Center, Vicksburg MS, USA
Clifton HE (1976) Wave-formed sedimentary structures – a conceptual model. In: Davis RA Jr, Ethington RL (eds) Beach and Nearshore Sedimentation. SEPM Spec Publ 24:126–148
Clifton HE, Dingler JR (1984) Wave-formed structures and paleoenvironmental reconstructions. Mar Geol 60:165–198
Collins JI (1976) Wave modelling and hydrodynamics. In: Davis RA Jr, Ethington RL (eds) Beach and Nearshore Sedimentation. SEPM Spec Publ 24:54–68
Davidson-Arnott R (2010) Introduction to Coastal processes and geomorphology. Cambridge University Press, Cambridge
Davies JL (1972) Geographical variation in Coastal Development. Oliver & Boayd, Edinburgh
Dean RG, Dalrymple RA (2004) Coastal processes – with Engineering Applications. Cambridge University Press, Cambridge
Dietz RS (1963) Wave-base, marine profile of equilibrium, and wave-built terraces: a critical appraisal. Geol Soc Am Bull 74:971–990
Flemming BW (2005) The concept of wave base: Fact and fiction. In: Haas H, Ramseyer K, Schlunegger F (eds) Abstracts. Sediment 2005, 18–20 July 2005, Gwatt, Lake Thun, Switzerland. Schriftenreihe der Deutschen Gesellschaft für Geowissenschaft 38, p 57
Hallermeier RJ (1978) Uses for a calculated limit depth to beach erosion. Coast Eng 1:1493–1512
Hallermeier RJ (1981) A profile zonation for seasonal sand beaches from wave climate. Coast Eng 4:253–277
Hamon-Kerivel K, Cooper A, Jackson D, Sedrati M, Guisado-Pintado E (2020) Shoreface mesoscale morphodynamics: a review. Earth-Sci Rev 209:103–330
Hardisty J (1994) Beach and nearshore sediment transport. In: Pye K (ed) Sediment Transport and depositional processes. Blackwell Science, Oxford, pp 219–255
Hobday DK, Reading HG (1972) Fair weather versus storm processes in shallow marine sandbar sequences in the late precambrian of Finnmark, North Norway. J Sediment Res 42:318–324
Horikawa K (1988) Nearshore Dynamics and Coastal processes: theory, measurement, and predictive models. University of Tokyo, Tokyo
Immenhauser A (2009) Estimating palaeo-water depth from the physical rock record. Earth-Sci Rev 96:107–139
Jackson DWT, Short AD (2020) Sandy Beach Morphodynamics. Elsevier, Amsterdam
Komar PD (1998) Beach Processes and Sedimentation (2nd edition). Prentice Hall, New Jersey
Komar PD, Miller MC (1973) The threshold of movement under oscillatory water waves. J Sediment Res 43:1101–1110
Le Roux JP An extension of the Airy theory for linear waves into shallow water. Komar PD, Miller MC (2008) (1973) The threshold of movement under oscillatory water waves. Coastal Engineering 55:295–301
Le Roux JP, Demirbilek Z, Brodalka M, Flemming BW (2010) WAVECALC: an Excel-VBA spreadsheet to model the characteristics of fully developed waves and their influence on bottom sediments in different water depths. Geo-Mar Lett 30:549–560
Masselink G, Hughes M, Knight J (2011) Introduction to Coastal processes and geomorphology (2nd Edition). Routledge, London
McCave IN (1971) Wave effectiveness at the sea bed and its relationship to bed-forms and deposition of mud. J Sediment Res 41:89–96
Pellegrini C, Sammartino I, Schieber J, Tesi T, Paladini de Mendoza F, Rossi V, Chiggiato J, Schroeder K, Gallerani A, Langone L, Trincardi F, Amorosi A (2023) On depositional processes governing along-strike facies variations of fine-grained deposits: unlocking the little ice age subaqueous clinothemes on the Adriatic shelf. Sedimentology. https://doi.org/10.1111/sed.13162
Peters SE, Loss DP (2012) Storm and fair-weather wave base: a relevant distinction? Geology 40:511–514
Rankey EC, Appendini CM (2022) Unfathomable: the shifting sand of wave base. J Sediment Res 92:95–111
Shepard FP (1963) Submarine geology. Harper & Row, New York
Short AD (ed) (1999) Handbook of Beach and Shoreface Morphodynamics. Wiley, Chichester
Son CS, Flemming BW, Chang TS (2012a) Sedimentary facies of shoreface-connected sand ridges off the East Frisian barrier-island coast, southern North Sea: climatic controls and preservation potential. IAS Spec Publ 44:143–158
Son CS, Flemming BW, Bartholomä A, Chun SS (2012b) Long-term changes in morphology and textural sediment characteristics in response to energy variation on shore-face-connected ridges off the East Frisian barrier-island coast, southern North Sea. J Sediment Res 82:385–399
Soulsby R (1997) Dynamics of Marine sands: a manual for practical applications. Thomas Telford, London
Valiente NG, Masselink G, Scott T, Conley D, McCarroll RJ (2019) Role of waves and tides on depth of closure and potential for headland bypassing. Mar Geol 407:60–75
Walker RG, Guy Plint A (1992) Wave- and storm-depositional shallow marine systems. In: Walker RG, James NP (eds) Facies models. Geol Soc Canada, pp 219–238
Wentworth CK (1922) A scale of grade and class terms of clastic sediments. J Geol 30:377–392
Wiberg PL, Sherwood C (2008) Calculating wave-generated bottom orbital velocities from surface-wave parameters. Comput Geosci 34:1243–1262
Woodborne M, Flemming B (2021) Sedimentological evidence for seiching in a swell-dominated headland-bay system: Table Bay, Western Cape, South Africa. Geo-Mar Lett 41:article46
Wright LD (1995) Morphodynamics of Inner Continental shelves. CRC, Boca Raton
Wright LD, Boon JD, Kim SC, List JH (1991) Modes of cross-shore sediment transport on the shoreface of the Middle Atlantic Bight. Mar Geol 96:19–51